First-in-Human Phase I/II ICONIC Trial of the ICOS Agonist Vopratelimab Alone and with Nivolumab: ICOS-High CD4 T-Cell Populations and Predictors of Response

Timothy A. Yap[1], Justin F. Gainor[2], Margaret K. Callahan[3], Gerald S. Falchook[4], Russell K. Pachynski[5], Patricia LoRusso[6], Shivaani Kummar[7], Geoffrey T. Gibney[8], Howard A. Burris[9], Scott S. Tykodi[10], Osama E. Rahma[11], Tanguy Y. Seiwert[12], Kyriakos P. Papadopoulos[13], Mariela Blum Murphy[1], Haeseong Park[5], Amanda Hanson[14], Yasmin Hashambhoy-Ramsay[14], Lara McGrath[14], Ellen Hooper[14], Xiaoying Xiao[14], Heather Cohen[14], Martin Fan[14], Daniel Felitsky[14], Courtney Hart[14], Rachel McComb[14], Karen Brown[14], Ali Sepahi[14], Judith Jimenez[14], Weidong Zhang[14], Johan Baeck[14], Haley Laken[14], Richard Murray[14], Elizabeth Trehu[14], and Christopher J. Harvey[14]

ABSTRACT

Purpose: The first-in-human phase I/II ICONIC trial evaluated an investigational inducible costimulator (ICOS) agonist, vopratelimab, alone and in combination with nivolumab in patients with advanced solid tumors.

Patients and Methods: In phase I, patients were treated with escalating doses of intravenous vopratelimab alone or with nivolumab. Primary objectives were safety, tolerability, MTD, and recommended phase II dose (RP2D). Phase II enriched for ICOS-positive (ICOS+) tumors; patients were treated with vopratelimab at the monotherapy RP2D alone or with nivolumab. Pharmacokinetics, pharmacodynamics, and predictive biomarkers of response to vopratelimab were assessed.

Results: ICONIC enrolled 201 patients. Vopratelimab alone and with nivolumab was well tolerated; phase I established 0.3 mg/kg every 3 weeks as the vopratelimab RP2D. Vopratelimab resulted in modest objective response rates of 1.4% and with nivolumab of 2.3%. The prospective selection for ICOS+ tumors did not enrich for responses. A vopratelimab-specific peripheral blood pharmacodynamic biomarker, ICOS-high (ICOS-hi) CD4 T cells, was identified in a subset of patients who demonstrated greater clinical benefit versus those with no emergence of these cells [overall survival (OS), $P = 0.0025$]. A potential genomic predictive biomarker of ICOS-hi CD4 T-cell emergence was identified that demonstrated improvement in clinical outcomes, including OS ($P = 0.0062$).

Conclusions: Vopratelimab demonstrated a favorable safety profile alone and in combination with nivolumab. Efficacy was observed only in a subset of patients with a vopratelimab-specific pharmacodynamic biomarker. A potential predictive biomarker of response was identified, which is being prospectively evaluated in a randomized phase II non–small cell lung cancer trial.

Introduction

Clinical benefit with single-agent programmed death-1 receptor or programmed death ligand-1 [PD-(L)1] inhibitors is limited to a minority of patients. There has been a substantial increase in combination trials investigating novel immunotherapy agents in combination with PD-(L)1 inhibitors, but few have been successful (1, 2). One approach to improve the value of these combination approaches is to determine the contributory effects of each agent through the implementation of pharmacodynamic biomarkers. Another strategy is to develop potential predictive biomarkers of response to identify patients most likely to benefit from the combination. The use of established predictive biomarkers, such as PD-L1 IHC, microsatellite instability (MSI)-high, and tumor mutational burden has contributed to improved clinical outcomes with PD-(L)1 inhibitors (3). However, there remains an unmet clinical need for the development of rational and effective combination regimens and identification of novel predictive biomarkers for the selection of appropriate patients for such therapies (4).

The inducible costimulator (ICOS) of T cells is a member of the B7/CD28/CTLA-4 immunoglobulin superfamily expressed largely on T cells. Unlike CD28, which is constitutively expressed on T cells, ICOS is upregulated following initial T-cell priming (5). Upon

[1]The University of Texas MD Anderson Cancer Center, Houston, Texas. [2]Massachusetts General Hospital, Boston, Massachusetts. [3]Memorial Sloan Kettering Cancer Center, New York, New York. [4]Sarah Cannon Research Institute at HealthONE, Denver, Colorado. [5]Washington University School of Medicine, St. Louis, Missouri. [6]Yale Cancer Center, New Haven, Connecticut. [7]Stanford University School of Medicine, Stanford, California. [8]Georgetown Lombardi Comprehensive Cancer Center, Washington, DC. [9]Sarah Cannon Research Institute, Nashville, Tennessee. [10]University of Washington and Fred Hutchinson Cancer Research Center, Seattle, Washington. [11]Dana-Farber Cancer Institute, Boston, Massachusetts. [12]University of Chicago, Chicago, Illinois. [13]South Texas Accelerated Research Therapeutics, San Antonio, Texas. [14]Jounce Therapeutics, Inc., Cambridge, Massachusetts.

Note: Supplementary data for this article are available at Clinical Cancer Research Online (http://clincancerres.aacrjournals.org/).

Corresponding Author: Timothy A. Yap, Department of Investigational Cancer Therapeutics (Phase I Program), The University of Texas MD Anderson Cancer Center, 1400 Holcombe Boulevard, Houston, TX 77030. Phone: 713-563-1784; E-mail: tyap@mdanderson.org

Clin Cancer Res 2022;XX:XX–XX

doi: 10.1158/1078-0432.CCR-21-4256

Translational Relevance

ICONIC demonstrated that vopratelimab, an inducible costimulator (ICOS) agonist mAb, was well tolerated alone and with nivolumab in patients with advanced solid tumors. Vopratelimab did not confer durable, antitumor activity nor did its combination with nivolumab improve efficacy in the majority of patients with advanced solid tumors. The prospective selection of patients with ICOS-positive tumors did not enrich for antitumor responses. However, reverse translational studies led to the identification of the emergence of peripheral ICOS-high CD4 T cells as a vopratelimab-specific pharmacodynamic biomarker. Furthermore, a potential predictive biomarker of response to vopratelimab alone and with a PD-1 inhibitor, comprising an RNA-based tumor inflammation signature with a specific threshold, was also identified. These findings are being prospectively validated in a randomized phase II non–small cell lung cancer trial.

activation, ICOS induces a signal through the PI3K/protein kinase B (AKT) pathway, resulting in the expression of lineage-specific transcription factors (e.g., T-bet, GATA-3) and subsequent T-cell proliferation and survival (6). Other T-cell costimulatory molecules such as OX40, 4-1BB, CD40, and CD28 have been shown to require ICOS signaling to exert their biological function, suggesting that ICOS regulates a critical nexus of costimulatory activity (7–11). Signaling through ICOS may also help overcome resistance to PD-(L)1–mediated T-cell exhaustion (12).

Signaling through ICOS leads to diverse effects on T-cell subsets, including proliferation, differentiation, and survival of distinct ICOS-high (hi) CD4 T-cell populations. Induction of a population of ICOS-hi CD4 T cells occurs upon treatment with the CTLA-4 antibody ipilimumab in PD-(L)1 inhibitor–naïve patients, and importantly, persistence of this T-cell population was associated with improved overall survival (OS) in patients with PD-1 inhibitor–naïve melanoma treated with ipilimumab (13). In preclinical models, treatment with ICOS agonist antibodies *in vivo* induced tumor regression in multiple tumor models and promoted long-term immunity (14). This antitumor activity was further enhanced in combination with anti-PD-1, suggesting ICOS agonist antibodies may enhance the effects of anti-PD-1 when administered in combination (14). In addition, ICOS antibody treatment led to an increase in frequency of CD8 T cells within mouse tumors; PD-(L)1 inhibitors restore effector CD8 T-cell activity, thus providing strong rationale for combining with a costimulator, such as an ICOS agonist (14).

Vopratelimab (JTX-2011) is an investigational potential first-in-class humanized IgG1κ agonist mAb that specifically binds to ICOS and is designed to augment an antitumor immune response (15). The mechanism of action of vopratelimab requires the initial priming of T cells followed by upregulation of ICOS expression on the cell surface of CD4 T cells, after which vopratelimab engagement results in their proliferation and sustained activation (14).

ICONIC, a phase I/II, open-label, multicenter, first-in-human (FIH) clinical trial, investigated the safety, tolerability, pharmacokinetics, pharmacodynamics, recommended phase II dose (RP2D), and preliminary efficacy of vopratelimab as monotherapy and in combination with nivolumab, as well as potential predictive biomarkers of response to therapy. Here we present the first publication of the ICONIC trial and detail how a pharmacodynamic biomarker for vopratelimab led to the identification of a potential predictive biomarker that is now being assessed prospectively in a phase II non–small cell lung cancer (NSCLC) clinical trial (SELECT, NCT04549025).

Patients and Methods

Study design

This four-part, adaptive phase I/II, open-label, multicenter, FIH trial was designed to evaluate the safety and tolerability, determine the MTD and RP2D, as well as the preliminary efficacy of the ICOS agonist mAb vopratelimab (JTX-2011) as monotherapy, and in combination with nivolumab in adult patients with advanced solid tumors (NCT02904226). Phase I was a classical 3+3 dose escalation that assessed escalating doses of vopratelimab (0.003–1.0 mg/kg) as monotherapy (part A) or in combination with fixed doses of nivolumab (part B). Parts A and B also included expansion cohorts (AP1, AP2, BP1, BP2) to further explore safety/pharmacokinetic/pharmacodynamic markers of vopratelimab alone and in combination with nivolumab.

In phase II, vopratelimab efficacy alone and in combination with nivolumab was investigated in specific tumors. Preclinical data suggested a high ICOS IHC score would be required for the optimal clinical benefit of an ICOS agonist; therefore, tumor types were selected on the basis of higher intratumoral ICOS expression. Vopratelimab treatment (part C) was assessed in PD-(L)1 inhibitor experienced head and neck squamous cell carcinoma (HNSCC) and NSCLC, PD-(L)1 inhibitor-naïve or experienced gastric or gastroesophageal junction cancer and PD-(L)1 inhibitor-naïve or experienced triple-negative breast cancer (TNBC), as well as other advanced solid tumors. Combined treatment with vopratelimab and nivolumab (part D) was assessed in PD-(L)1 inhibitor experienced HNSCC and NSCLC, and PD-(L)1 inhibitor naïve and experienced TNBC and gastric or gastroesophageal junction cancer. PD-(L)1 inhibitor–experienced tumors were defined as cancers that have progressed on or after therapy with a PD-1 or PD-L1 inhibitor.

Part C enriched for patients with medium to high ICOS expression per IHC score in archival tumor, with ICOS levels reassessed on a fresh pretreatment biopsy. At least 10 patients with ICOS-hi tumors by IHC on a fresh biopsy and at least 5 patients with ICOS-low (ICOS-lo) tumors by IHC on a fresh biopsy were required in each part C cohort. Part D enrolled indications anticipated to have ICOS-positive tumors (NSCLC, HNSCC, gastric, and TNBC). ICOS expression levels vary within these indications; therefore, patients were stratified for ICOS expression.

Both phases examined the correlation between potential predictive biomarkers of response and efficacy [response rate, duration of response (DoR), disease control rate (DCR), landmark progression-free survival (PFS) rate, PFS, landmark OS rate, and OS] as exploratory objectives.

Patients

Patients were enrolled from 16 sites in North America from August 2016 to May 2018. All were required to have evaluable or measurable disease, according to RECIST v1.1, with at least one measurable lesion. All enrolled patients were ≥18 years of age, had an Eastern Cooperative Oncology Group performance status ≤1, and a predicted life expectancy ≥3 months. Measurable disease was required for phase II.

Dose-escalation cohorts included patients with advanced and/or refractory, non-hematologic, extracranial malignancy with disease progression after treatment with all available therapies known to confer clinical benefit. For phase II cohorts, patients must have progressed on or after all approved therapies. Patients who were

receiving concurrent anticancer treatment, had refused standard therapy, were immunodeficient, were receiving immunosuppressive therapy, or had undergone major surgery <6 weeks prior to the first data of study treatment, were excluded. Further information regarding inclusion and exclusion criteria is available at clinicaltrials.gov (NCT02904226). The study was conducted in accordance Good Clinical Practice guidelines defined by the International Conference on Harmonization. Approval was obtained from independent ethics committees and Institutional Review Boards at all participating centers and all patients provided informed written consent prior to participation based on the principles of the Declaration of Helsinki.

Interventions

Patients were treated with vopratelimab monotherapy (JTX-2011; a humanized IgG1κ mAb and ICOS agonist; Jounce Therapeutics, Inc.), or vopratelimab in combination with nivolumab (OPDIVO; a human IgG4κ anti-PD-1 mAb; Bristol-Myers Squibb). All study drugs were administered intravenously every 3 weeks.

In the dose escalation (parts A and B), vopratelimab monotherapy was dosed from 0.003 mg/kg escalating to 1.0 mg/kg; nivolumab was dosed at 240 mg i.v. every 3 weeks. Vopratelimab in combination with nivolumab was dosed from 0.01 mg/kg escalating to 0.3 mg/kg. Dose escalation was approved by a Safety Monitoring Committee composed of investigators and sponsor representatives at each stage. In the phase II efficacy cohorts (C and D), vopratelimab was administered at the RP2D determined from the phase 1 dose escalation (0.3 mg/kg i.v. every 3 weeks), and nivolumab was administered at 240 mg/kg i.v. every 3 weeks.

Efficacy assessment

Antitumor activity was investigator assessed using RECIST v1.1, and imaging for efficacy assessments was performed approximately every 9 weeks by CT. PFS (per RECIST 1.1 investigator assessment) was defined as the number of months from the date of first dose to the date of death or documented (objective) disease progression via RECIST v1.1 by investigator assessment, whichever occurred sooner. OS was defined as the interval of time from first dose date to the date of death for any cause.

Pharmacokinetics of vopratelimab and nivolumab

Blood samples were collected for vopratelimab concentration determinations during cycle 1 prior to dosing, at 0.5, 1, 1.5 (vopratelimab monotherapy), or 2.5 (vopratelimab in combination with nivolumab), 4 and 6 hours postdose, and 2, 8, and 15 days postdose. For subsequent cycles, samples were collected predose and 1 hour postdose. All times were relative to the start of the vopratelimab infusion times. Blood samples for nivolumab concentration determinations were collected at the same timepoints as for vopratelimab.

Vopratelimab concentrations were quantified in serum using a validated electrochemiluminescent assay. Briefly, vopratelimab was captured on meso scale discovery (MSD) plates coated with a mouse anti-human vopratelimab mAb. Detection was via the same mAb conjugated to ruthenium. The assay was validated to a lower limit of quantitation (LLOQ) of 750 pg/mL.

Nivolumab concentrations were measured in serum using a validated ELISA. Briefly, nivolumab was captured on 96-well plates coated with either PD-1-human IgG1 fusion protein or his-tagged recombinant PD-1 protein and detected using a mouse anti-human IgG4 mAb conjugated to horseradish peroxidase (HRP). The assay was validated to an LLOQ of 100 ng/mL.

Samples for vopratelimab anti-drug antibodies (ADA) and neutralizing ADA were collected predose on day 1 of each cycle. ADA to vopratelimab were detected via an electrochemiluminescent assay using a three-tier procedure that consisted of screening without added vopratelimab, screening with added vopratelimab to confirm specificity, and serial dilution of positive samples to determine the titer. Briefly, clinical samples or controls were diluted 1:50 into acetic acid to disrupt existing ADA/drug complexes, then incubated with a neutralizing solution containing biotinylated vopratelimab (bt-vopratelimab) and ruthenium-labeled vopratelimab (ru-vopratelimab). For specificity screening and titering, unlabeled vopratelimab was also included in the assay solution. Bridging complexes of bt-vopratelimab-ADA-ru-vopratelimab were captured on streptavidin-coated plates and ru-vopratelimab was quantitated by electrochemiluminescence. Samples testing positive in both screening steps were considered positive and corresponding titers were determined by serial dilution and reported. Otherwise, samples were reported as negative.

ADA-positive samples were further assayed for neutralizing activity. Briefly, samples were acid treated, then incubated with bt-vopratelimab in a neutralizing buffer. The resulting complexes were captured on a streptavidin-coated plate, washed, and then acid treated to dissociate ADA. The acid-treated samples were incubated with ru-vopratelimab in neutralizing buffer, transferred to an MSD-streptavidin plate coated with biotin-conjugated ICOS to capture uncomplexed ru-vopratelimab. Captured ru-vopratelimab was quantitated by electrochemiluminescence. A maximal signal was observed in absence of neutralizing ADA, and the amount of neutralizing activity was estimated on the basis of the decline in signal.

Pharmacokinetic parameters were calculated for vopratelimab and nivolumab for cycle 1 by noncompartmental analysis using Phoenix WinNonlin (v. 8.2). C_{max}, C_{trough}, and the AUC from the start of dosing to the last measured timepoint (AUC_{last}) were calculated for all patients. For patients treated with nivolumab, the AUC from dosing through day 14 was also calculated for comparison with historical data for nivolumab administered every 2 weeks. When the data were adequate to estimate the terminal elimination half-life, half-life values were also reported for vopratelimab. Actual sampling times were used for the analysis. C_{max}, C_{trough}, and AUC values were summarized by geometric mean and geometric coefficient of variation. Half-life was summarized by arithmetic mean and SD.

Samples analyzed for immunophenotyping studies

Blood collections and peripheral blood mononuclear cell (PBMC) processing from clinical samples were performed at clinical sites. Patient blood was collected directly into 8 mL sodium heparin CPT tubes using a BD vacutainer safety-lok blood collection system and processed according to manufacturer's instructions with the following modifications. Immediately after collection the CPT tube was gently inverted 10 times to mix the anticoagulant with the blood. CPT tubes were then spun at 1,800 × *g* for 15 minutes at 22°C in a swing bucket centrifuge, cell and plasma fractions were then decanted into a 15 mL Falcon tube and spun at 300 × *g* for 15 minutes at 22°C. Supernatant was decanted, and the cell pellet was resuspended in 1 mL freezing media (10% FBS in DMSO) and transferred via pipet to a 1.8 mL cryovial. Cryovials were immediately placed in a room temperature Mr. Frosty (Thermo Fisher Scientific) or CoolCell (Corning) and stored overnight in a −80°C freezer and then shipped directly to Jounce or FlowMetric packed in dry ice. Upon arrival to Jounce or FlowMetric, cryovials were immediately stored at −80°C until flow cytometry analysis.

In a companion study, cryopreserved PBMC samples from anti-PD-1/L1 inhibitor monotherapy-treated patients were purchased from Discovery Life Sciences. Upon receipt, all samples were stored at −80°C until flow cytometry analysis.

Immunophenotyping of PBMC samples

ICOS-hi $CD4^+$ T-cell immunophenotyping

PBMCs were counted and 1×10^6 cells were resuspended in flow buffer (PBS+2% FBS, 1 mmol/L EDTA, and 0.1% sodium azide) containing CD3-APC-H7 (clone SK7, BD Biosciences) and CD4-PerCP-Cy5.5 antibodies (clone L200, BioLegend) for 30 minutes at 4°C. After washing with flow buffer, cells were permeabilized and fixed using the FOXP3 Fixation/Permeabilization Concentrate and Diluent Kit (eBioscience) according to the manufacturer's instructions. Permeabilized cells were stained with biotinylated anti-human ICOS antibody (clone: M13, Jounce Therapeutics, a noncompetitive binder to ICOS compared with vopratelimab) for 30 minutes at 4°C. After washing, cells were incubated with streptavidin-PE (BioLegend) for 30 minutes at 4°C, washed and then resuspended in flow buffer. In some experiments, Tbet-BV421 (clone 4B10, BioLegend) was added at the intracellular staining step.

Flow cytometry was performed on the same day using the FACSCanto II or LSR Fortessa (BD).

After January 2019, all clinical samples were analyzed at FlowMetric. The same method, flow panel, and analysis were followed at both Jounce and FlowMetric.

ICOS-hi versus ICOS-lo emergence criteria

Peripheral CD4 T cells were identified as ICOS-hi or ICOS-lo based on predetermined flow cytometry parameters that were established individually for each subject at baseline. ICOS-hi and ICOS-lo gates were drawn based on isotype stain and baseline samples, respectively. Mean fluorescence intensity (MFI) and % of CD4 T cells above baseline were reported for each sample. For a subject to be classified as "ICOS-hi," ≥5% of ICOS-stained cells had to exhibit a ≥1.5-fold increase over baseline MFI for at least one postdose visit. A patient was placed in the ICOS-lo group if they did not meet the criteria for ICOS-hi and had at least one evaluable peripheral blood CD4 T-cell sample postbaseline. Emergence of ICOS-hi CD4 T cells was observed mid-way through the study with most samples analyzed retrospectively. Samples were collected at specific visits outlined in the study protocol though evaluable samples were not available at every timepoint.

IHC for ICOS and PD-L1 predictive biomarkers

PD-L1 and ICOS levels were evaluated in archival and pretreatment tumor biopsies by NeoGenomics Laboratories Inc. ICOS was reported by a score of 0, 1, 2 or 3, while PD-L1 was evaluated using a tumor proportion score.

For the detection of ICOS, samples were baked for 1 hour at 60°C. The slides were then processed on an automated IHC stainer (BOND, Leica Biosystems). Briefly, slides were dewaxed, incubated in 100% alcohol, and rinsed in wash buffer. Antigen retrieval was performed using the BOND ER2 solution at 100°C for 25 minutes. Slides were rinsed in wash buffer, followed by a peroxide block for 10 minutes, and then rinsed again in wash buffer. A protein block was then applied for 30 minutes, followed by 0.5 mg/mL anti-ICOS (clone M13) for an additional 30 minutes. Slides were then rinsed in wash buffer, followed by protein block for another 30 minutes. Slides were incubated with postprimary antibody (Leica) for 8 minutes, then rinsed in wash buffer, followed by incubation in HRP polymer for 8 minutes. Slides were rinsed in wash buffer, followed by deionized water, and then in 3,3′-diaminobenzidine chromogen solution for 10 minutes. Slides were rinsed in deionized water, then incubated with hematoxylin counterstain for 7 minutes. Slides were then rinsed in deionized water, followed by wash buffer, and then deionized water again. Slides were dehydrated through graded alcohol and xylene, prior to applying coverslips. All reagents were provided by Leica Biosystems, Germany unless otherwise stated.

For the detection of PD-L1, the 22C3 PharmDX assay was utilized using an Autostainer Link 48. Briefly, slides were incubated in target retrieval solution for 20 minutes at 97°C, followed by cooling to 65°C. Slides were then incubated in EnVision FLEX Wash Buffer at room temperature for 5 minutes, and transferred to the autostainer for the automated PD-L1 IHC 22C3 protocol. Once staining was complete, the slides were counterstained with EnVision FLEX Hematoxylin (Agilent-DAKO), prior to applying coverslips. All equipments, kits, and reagents were provided by Agilent Technologies, Inc, unless otherwise stated.

For both IHC assays, appropriate controls were used to evaluate assay performance. For ICOS, this included both positive and negative cell lines, as well as a positive tonsil tissue. For PD-L1, control tissues were utilized as indicated in the 22C3 PharmDX assay manual (Dako, Agilent Technologies, Inc.), including gastric adenocarcinoma or NSCLC as appropriate. For indications not covered by the 22C3 PharmDX assay manual, controls included universal laboratory controls (placenta, smooth muscle), along with the PD-L1 IHC 22C3 Control Cell Line Slides (Dako, Agilent Technologies, Inc.).

Analysis of gene expression using NanoString

Four slices from each pretreatment formalin-fixed paraffin-embedded tumor block were cut and used for RNA extraction using the High Pure RNA Paraffin Kit (catalog no. 03 270 289 001, Roche) as per the manufacturer's recommendations. Quality and quantity were observed with the 5200 Fragment Analyzer system (Agilent Technologies Inc.) in conjunction with the highsensitivity RNA Kit (15NT; catalog no. DNF-472, Agilent Technologies Inc.). If sufficient RNA was present, 50 ng of RNA was processed according to the manufacturer's instructions for the NanoString nCounter workflow (two reactions contained 45 and 30 ng, due to low yield). All samples were evaluated using a custom-designed base sequence (Jounce Therapeutics, Inc.), nCounter panel, as well as custom-designed indication-specific spike-in panels, where appropriate. Samples were profiled on an nCounter SPRINT Profiler (NanoString Technologies Inc.).

Patient samples utilized for gene expression (tumor inflammation signature) evaluation

Data from fresh pretreatment biopsies from 89 patients that passed NanoString's quality control described above were assessed: 29 patients were treated with vopratelimab monotherapy, while 60 were treated with vopratelimab in combination with nivolumab. Tumor samples obtained were from the safety/pharmacokinetic/pharmacodynamic expansion cohorts AP1/AP2 ($n = 8$) and BP1/BP2 ($n = 14$) and phase II efficacy cohorts C ($n = 21$) and D ($n = 46$). See Supplementary Fig. S10 for disposition of tumor tissue samples analyzed for tumor inflammation signature (TIS).

Evaluation of gene expression data—TIS scores

Raw .RCC files were submitted to NanoString Technologies, Inc., data analysis service, to calculate the TIS score. All 28 genes (18 immune and 10 housekeeping) were included in the Jounce custom nCounter panel. Scores were calculated by normalizing to TIS reference sample (*in vitro* transcripts specific for each TIS genes of a known

concentration), followed by housekeeping genes and applying weights specified in (16). Only samples that passed NanoString's signal quality control were included in further analysis.

Individual genes were evaluated for their ability to predict the emergence of the pharmacodynamic biomarker. Raw gene expression data were processed by removing poor quality samples, then normalizing the remaining samples to housekeeping genes. Genes that were measured across all samples were included in analysis. Gene expression was compared between the group of patients who showed emergence of ICOS-hi $CD4^+$ T cells and the group of patients who did not display the emergence of this population.

Gene expression profiling of ICOS-hi $CD4^+$ T cells

Transcriptional profiles of peripheral blood $CD4^+$ T cells from patients who demonstrated emergence of ICOS-hi $CD4^+$ T cells were compared with $CD4^+$ T cells from representative cancer patient samples in which ICOS-hi CD4 T cells were not detected. From these samples, $CD4^+$ T cells were separated by magnetic columns, and total RNA was extracted and processed using the nCounter Human Immunology Panel (NanoString Technologies Inc). Differential gene expression was compared between vopratelimab patients and donor samples by unpaired *t* tests and corrected for FDS using the Benjamini–Hochberg procedure.

Predictive biomarker assessment

TIS score, PD-L1 IHC, and ICOS IHC based on pretreatment tumor samples, and ICOS IHC and PD-L1 IHC based on archival tumor samples were evaluated for their suitability as predictive biomarkers for pharmacodynamic response (ICOS-hi $CD4^+$ T-cell emergence) and efficacy response in patients treated with vopratelimab monotherapy or vopratelimab and nivolumab combination therapy. Details of assessment methods can be found in the Statistical analysis section.

Statistical analysis

Results are summarized via summary statistics (number, mean, median, SD, quartiles, minimum, maximum for continuous endpoints; number and percent for binary and categorical endpoints). The correlation between efficacy and potential predictive biomarkers was explored to generate hypotheses for further testing. All data analyses were conducted using the SAS System (SAS Institute, Inc., RRID: SCR_008567) Version 9.4. Volcano plots, box plots and IHC histograms were plotted using TIBCO Spotfire version 7.11.1.0.12.

For the evaluation of gene expression data, statistics were calculated in R*; specifically, *t* tests were performed using the "t.test" function, and nominal *P* values, adjusted *P* values (using the Benjamini–Hochberg method) and average fold changes were calculated.

*{R: A Language and Environment for Statistical Computing}, author = {{R Core Team}}, organization = {R Foundation for Statistical Computing}, address = {Vienna, Austria}, year = {2018}, url = {https://www.R-project.org/}

Detailed statistics for predictive biomarkers

ROC curves were used to evaluate the ability of biomarkers to predict ICOS-hi $CD4^+$ T-cell emergence. The ROC curves for each biomarker were plotted with the true positive rate (sensitivity) against the false positive rate (1 − specificity) using all observed values as cut-off values. AUC was also calculated for a measure of the average accuracy for the biomarker prediction. Youden Index was calculated for each ROC curve over the possible cut-off values as follows: Youden index = Sensitivity + Specificity − 1 (the cut-off value which maximizes Youden index was chosen as the best cutoff). After a predictive biomarker and its cutoff were chosen using ROC curve and Youden index as above, efficacy evaluations were provided by biomarker subgroups as separated by the cutoff (e.g., TIS positive and TIS negative subgroups).

Waterfall plots were used to display maximum percent change from baseline in tumor measurements (measurements in sum of diameters of target tumors) with colors indicating biomarker subgroups. Swimmer plots of time on treatment were also provided for patients who were evaluated for TIS score with separate panels for patients who are TIS^{vopra} positive and TIS^{vopra} negative. Estimates of PFS and OS were summarized using the Kaplan–Meier method (17), with median and corresponding two-sided 95% confidence interval (CI) by biomarker subgroups (predictive biomarker selected using steps above).

Sample size

For the dose-escalation studies, the exact sample size was not predetermined because of the dynamic nature of the classical 3+3 design. For phase II tumor-specific expansion cohorts, a group sequential design was considered for sample size determination [Jennison and Turnbull, 2000. reference: Group Sequential Methods with Applications to Clinical Trials (Chapman & Hall/CRC Interdisciplinary Statistics) 1st Edition]. A 90% power at a two-sided α of 5% was designed to be achieved for the hypothesis testing by enrolling approximately 15 patients per cohort (no more than 2% of β spent at interim) as the first step, and a potential expansion up to approximately 49 patients per cohort if the futility boundary is passed on the basis of the results from the first 15 patients for each cohort.

Part D (vopratelimab + nivolumab) opened to enrollment shortly after part C (vopratelimab monotherapy). Patients were preferentially enrolled into the combination cohort for a total of 100 patients in part D. Lack of efficacy was observed with vopratelimab as a single agent, hence part C was closed to enrollment after a total of 30 patients.

Data availability

All data relevant to the article are contained within the main and Supplementary Data. Source/raw data for transcriptomic analysis are available upon request.

Results

A total of 201 patients with various advanced solid tumors who progressed on or after all approved therapies were enrolled and treated with either vopratelimab monotherapy or vopratelimab in combination with nivolumab on the ICONIC trial. As shown in **Table 1**, patients received a median of three prior lines of therapy in the metastatic setting (range, 0–12) and all were included in the safety analysis set (Supplementary Fig. S1); 187 (93%) patients met the criteria to be considered evaluable for efficacy (Supplementary Fig. S1) as they completed a baseline tumor assessment and either had at least one postbaseline tumor assessment scan and/or discontinued treatment due to death or disease progression. A total of 167 (83%) of these evaluable patients had at least one on-treatment tumor assessment.

In the phase I dose-escalation portion, 71 patients were enrolled and treated with vopratelimab alone ($n = 40$) or in combination with nivolumab ($n = 31$) at escalating doses of 0.003, 0.01, 0.03, 0.1, 0.3, and 1 mg/kg every 3 weeks. In phase II, 130 patients were enrolled and treated with vopratelimab alone ($n = 30$) or in combination with nivolumab ($n = 100$). In phase II, vopratelimab was administered intravenously at 0.3 mg/kg every 3 weeks, the RP2D defined during

Table 1. Patient demographics (data cutoff: 07-22-2020).

ICONIC patient characteristics	Vopratelimab monotherapy Total *n* = 70 (%)	Vopratelimab + nivolumab Total *n* = 131 (%)
Age (yrs), median (range)	64.0 (23.8–81.1)	60.0 (28.9–85.3)
Male	35 (50.0)	73 (55.7)
Female	35 (50.0)	58 (44.3)
Caucasian	51 (72.9)	99 (75.6)
Non-Caucasian	13 (18.6)	19 (14.5)
Not reported or missing	6 (8.6)	13 (9.9)
Prior therapies, median	3.0	3.0
≥3 prior therapies, *n* (%)	56 (80.0)	83 (63.4)
Prior immunotherapy, *n* (%)	32 (45.7)	67 (51.1)
Refractory to prior immunotherapy (best overall response of progressive disease), *n* (%)	14/32 (20.0)	25/67 (19.1)
Tumor type, *n* (%)	Gastric *n* = 10 (14.3) NSCLC *n* = 7 (10.0) TNBC *n* = 8 (11.4) HNSCC *n* = 6 (8.6) Other *n* = 39 (55.7) Bile duct *n* = 1, bladder *n* = 1, breast *n* = 1, cholangiocarcinoma *n* = 1, colon *n* = 4, endometrial *n* = 4, HNSCC[a] *n* = 5, melanoma *n* = 4, neuroendocrine *n* = 1, origin unknown *n* = 1, ovarian *n* = 2, pancreatic *n* = 2, peritoneum *n* = 1, prostate *n* = 2, rectal *n* = 2, renal *n* = 2, sarcoma *n* = 4, TNBC[a] *n* = 1	Gastric *n* = 35 (26.7) NSCLC *n* = 17 (13.0) TNBC *n* = 29 (22.1) HNSCC *n* = 26 (19.8) Other *n* = 24 (18.3) Breast *n* = 2, cervical *n* = 2, colon *n* = 4, endometrial *n* = 3, HNSCC[a] *n* = 3, melanoma *n* = 3, ovarian *n* = 1, pancreatic *n* = 1, prostate *n* = 1, rectal *n* = 2, sarcoma *n* = 2

Abbreviations: HNSCC, head and neck squamous cell carcinoma; NSCLC, non–small cell lung cancer; SD, standard deviation; TNBC, triple-negative breast cancer.
[a]These HNSCC and TNBC tumors were evaluated for efficacy with "Other."

phase I based on safety, pharmacokinetics, and sustained target engagement through the 3-week dosing period (see Pharmacokinetics, immunogenicity, and receptor occupancy of vopratelimab section).

Safety and tolerability

Vopratelimab administered as monotherapy and in combination with nivolumab was well tolerated in both the phase I and phase II portions of the study. The dose escalation established a MTD of 0.3 mg/kg i.v. every 3 weeks for vopratelimab, after two dose-limiting toxicities (DLT) were observed at 1.0 mg/kg, one dose level above the RP2D. The DLTs were assessed as being inflammatory and consistent with the mechanism of action of vopratelimab; these included a grade 3 aspartate aminotransferase (AST)/alanine aminotransferase elevation, which resolved with steroids within 72 hours and a grade 3 rapid worsening of a pleural effusion that was present at baseline.

Of the patients treated with vopratelimab monotherapy, 96% experienced a grade 1–2 treatment-emergent adverse event (TEAE), while 56% experienced grade 3–4 (Supplementary Table S1). The most common grade 3–4 TEAEs observed included: anemia (11.4%), hyponatremia (8.6%), diarrhea (5.7%), and elevated AST levels (5.7%). A total of 97% of those treated with vopratelimab and nivolumab experienced a grade 1–2 TEAE, while 48% experienced grade 3–4. The most frequent grade 3–4 TEAEs observed with combination treatment included hyponatremia (9.9%), anemia (5.3%), elevated AST (4.6%), and increased blood bilirubin (4.6%; Supplementary Table S1).

As listed in **Table 2**, grade 1–2 treatment-related AEs (TRAEs) were observed in 61% of patients receiving vopratelimab monotherapy, the most common being fatigue (13%), decreased appetite (10%), nausea (8.6%) and infusion-related reaction (8.6%). Grade 3–4 TRAEs were observed in 14% and included diarrhea (4.3%), anemia (4.3%), and increased AST (2.9%). In patients who received combination therapy, 76% experienced grade 1–2 and 11.5% grade 3–4. The most common grade 1–2 TRAEs were nausea (21.4%), infusion-related reaction (19.1%), fatigue (17.6%) and decreased appetite (13.7%). The most common grade 3–4 TRAEs included increased AST (3.1%), hyponatremia (1.5%), maculopapular rash (0.8%), and abdominal pain (0.8%).

In ICONIC, 12.9% of patients treated with vopratelimab monotherapy experienced an immune-related AE (irAE) while 25.5% of patients treated with vopratelimab plus nivolumab reported an irAE. The most common were anemia and rash for both vopratelimab alone and with nivolumab, and all cases were mild to moderate. No significant irAEs were observed as they relate to anemia, hyponatremia, or other endocrinopathies.

Because vopratelimab is an IgG1 molecule, analysis of peripheral blood immune cell subsets to rule out immune cell depletion was included in the safety evaluation, and no significant changes were observed in CD4 T effector cells, CD4 regulatory T cells, CD8 T cells, or natural killer cells (Supplementary Fig. S2).

Pharmacokinetics, immunogenicity, and receptor occupancy of vopratelimab

Pharmacokinetic parameters, calculated by noncompartmental analysis after the first dose of vopratelimab from the phase I dose escalation and expansion cohorts, are summarized in Supplementary Table S2. Target-mediated drug disposition was apparent at doses below 0.03 mg/kg. The appearance of both ADA and neutralizing ADA were transient in many patients, not dose dependent, and there was no apparent effect of ADA or neutralizing ADA on the pharmacokinetics of vopratelimab. Specifically, treatment-induced

Table 2. TRAEs (data cutoff: 07-22-2020).

	Vopratelimab monotherapy		Vopratelimab + nivolumab	
	N = 70 (%)		*N* = 131 (%)	
Preferred term	**Grade 1 and 2** ***n*** **(%)**	**Grade ≥3** ***n*** **(%)**	**Grade 1 and 2** ***n*** **(%)**	**Grade ≥3** ***n*** **(%)**
Patients with at least one TRAE	43 (61.4)	10 (14.3)	100 (76.3)	15 (11.5)
Nausea	6 (8.6)	0	28 (21.4)	0
Fatigue	9 (12.9)	0	23 (17.6)	0
Infusion-related reaction	6 (8.6)	1 (1.4)	25 (19.1)	0
Decreased appetite	7 (10.0)	0	18 (13.7)	0
Chills	4 (5.7)	0	11 (8.4)	0
Pyrexia	4 (5.7)	0	11 (8.4)	0
Aspartate aminotransferase increased	1 (1.4)	2 (2.9)	6 (4.6)	4 (3.1)
Diarrhea	4 (5.7)	3 (4.3)	9 (6.9)	0
Pruritus	6 (8.6)	0	5 (3.8)	0
Rash	4 (5.7)	0	7 (5.3)	0
Arthralgia	1 (1.4)	0	8 (6.1)	0
Vomiting	1 (1.4)	0	8 (6.1)	0
Constipation	1 (1.4)	0	7 (5.3)	0
Myalgia	0	0	8 (6.1)	0
Alanine aminotransferase increased	2 (2.9)	1 (1.4)	4 (3.1)	0
Headache	1 (1.4)	0	6 (4.6)	0
Rash maculopapular	0	0	7 (5.3)	1 (0.8)
Anemia	3 (4.3)	3 (4.3)	1 (0.8)	0
Blood alkaline phosphatase increased	0	0	4 (3.1)	0
Cough	0	0	5 (3.8)	0
Dizziness	4 (5.7)	0	1 (0.8)	0
Dyspnea	2 (2.9)	0	3 (2.3)	0
Hyponatremia	0	0	4 (3.1)	2 (1.5)
Hypothyroidism	0	0	5 (3.8)	0
Asthenia	0	1 (1.4)	3 (2.3)	0
Musculoskeletal pain	1 (1.4)	0	3 (2.3)	0
Weight decreased	1 (1.4)	0	3 (2.3)	0
Abdominal pain	0	0	2 (1.5)	1 (0.8)
Dehydration	2 (2.9)	0	1 (0.8)	0
Dry mouth	1 (1.4)	0	2 (1.5)	0
Dry skin	1 (1.4)	0	2 (1.5)	0
Flushing	1 (1.4)	0	2 (1.5)	0

Note: TRAEs include those with possible, probable, or missing relationship to any study drug.

ADA to vopratelimab across phase I and phase II were detected in up to 24.5% of patients with vopratelimab monotherapy and up to 34.5% of patients with vopratelimab plus nivolumab. Treatment-boosted ADAs were detected in up to 2.7% of patients treated with vopratelimab monotherapy and up to 8.0% of patients treated with vopratelimab plus nivolumab. The frequency of neutralizing ADA was lower: up to 8.1% with vopratelimab monotherapy and up to 13.8% with the combination. There was no apparent difference between vopratelimab pharmacokinetic parameters determined by noncompartmental analysis for patients with and without ADA, and a concentration–response relationship between vopratelimab exposure and target engagement was established. The RP2D of vopratelimab, 0.3 mg/kg every 3 weeks, was selected because it did not exceed the MTD and resulted in concentrations that achieved or exceeded concentrations necessary to achieve complete receptor occupancy (defined as >70% binding of ICOS) throughout the dosing interval (Supplementary Fig. S3).

Pharmacokinetics of vopratelimab + nivolumab

Nivolumab was administered at 240 mg i.v. every 3 weeks; this dose schedule was investigational at the time the study was open and coincided with that of vopratelimab. Where applicable, the maximum observed concentration (C_{max}) and AUC of nivolumab over the first 14 days of cycle 1 are presented in Supplementary Table S2. Nivolumab AUC values over the first 14 days after administration were comparable with previously reported values (18), and there was no apparent effect of vopratelimab coadministration on nivolumab C_{max} or AUC. Likewise, nivolumab had no apparent effect on the cycle 1 pharmacokinetics of vopratelimab.

Preliminary efficacy

The efficacy of vopratelimab, both as monotherapy and in combination with nivolumab, was evaluated for all tumors, as well as each of the four tumor-specific cohorts in phase II (gastric cancer, NSCLC, HNSCC, and TNBC), overall and according to baseline tumor ICOS IHC and PD-L1 scores. Preliminary efficacy results (**Table 3**) represent all patients with these tumor types from phase I ($n = 57$) and phase II ($n = 110$). Vopratelimab monotherapy demonstrated a confirmed investigator-assessed RECIST v1.1 partial response (PR) in 1 patient with advanced gastric cancer who was PD-(L)1 naïve. Vopratelimab in combination with nivolumab demonstrated confirmed RECIST v1.1 PRs in 2 of 35 patients with advanced gastric cancer [5.7%; 17% PD-(L)

Table 3. Preliminary efficacy of vopratelimab as monotherapy or in combination with nivolumab (phase I and phase II) data cutoff: 07-22-2020.

	Gastric		NSCLC		TNBC		HNSCC		Other		All/Total	
	Vopra	Vopra + nivo	Vopra	Vopra + nivo	Vopra	Vopra + nivo	Vopra	Vopra + nivo	Vopra	Vopra + nivo	Vopra	Vopra + nivo
Patients, *n*	10	35	7	17	8	29	6	26	39	24	70	131
Prior PD-(L)1i, *n*	2	6	7	17	1	6	6	26	14	10	30	65
PR+CR [# patients (ORR)]	1 (10.0%)	2 (5.7%)	0	0	0	1 (3.4%)	0	0	0	0	1 (1.4%)	3 (2.3%)
DCR, *n* (%)	2 (20.0%)	11 (31.4%)	0	5 (29.4%)	1 (12.5%)	4 (13.8%)	2 (33.3%)	3 (11.5%)	5 (12.8)	7 (29.2)	10 (14.3)	30 (22.9)
Median PFS (months) (95% CI)	2.1 (0.7–3.5)	2.1 (1.8–3.1)	1.9 (1.4–2.2)	1.9 (1.7–3.4)	2.1 (1.3-NE)	1.8 (1.3–2.0)	2 (1.1–2.1)	2 (1.8–2.1)	2 (1.9–2.1)	2 (1.8–3.9)	2 (1.9–2.1)	2 (1.9–2.0)
Median OS (months) (95% CI)	7.5 (1.8–10.8)	5.7 (3.1–9.8)	3.4 (2.3–11.2)	12.3 (6.3–16.9)	7.3 (1.7–7.7)	7.8 (4.6–11.3)	9.2 (4.9–9.2)	10.9 (6.2–15.8)	7.5 (3.9–10.5)	12.2 (6.6–13.2)	7.5 (4.9–9.2)	9.0 (7.2–11.7)

Abbreviations: DCR, disease control rate - confirmed CR or PR + stable disease lasting at least 53 days; HNSCC, head and neck squamous cell carcinoma; NE, not estimable; NSCLC, non-small cell lung cancer; ORR, overall response rate - confirmed CR or PR; PD-(L)1i, PD-(L)1 inhibitor; TNBC, triple-negative breast cancer.

1 inhibitor experienced] and in 1 of 29 (3.4%) patients with advanced TNBC [21% PD-(L)1 inhibitor experienced]; all responders were PD-(L)1 naïve, and each of these responses were highly durable: 1 for almost 3.5 years; 2 are ongoing after 4 years. No RECIST v1.1 responses were observed with monotherapy or combination therapy in patients with other tumors or PD-(L)1 inhibitor experienced HNSCC or NSCLC (Supplementary Fig. S4). The median PFS for the total population was 2.0 months (95% CI, 1.9–2.1 for vopratelimab monotherapy; 95% CI, 1.9–2.0 for vopratelimab in combination with nivolumab). The median OS for the entire population was 7.5 months (95% CI, 4.9–9.2) for those in the vopratelimab monotherapy group and 9.0 months (95% CI, 7.2–11.7) in the combination group (**Table 3**; Supplementary Fig. S5). In both treatment groups, there were no apparent associations of clinical outcomes with either ICOS IHC or PD-L1 IHC in the baseline tumor (Supplementary Table S3).

Identification of a vopratelimab-specific pharmacodynamic biomarker

To investigate mechanisms underlying the clinical outcomes, PBMC samples were analyzed from a subset of 44 patients who had both longitudinal PBMC samples with sufficient viable cells and were evaluable for efficacy, including the 4 responders. This analysis of cellular changes by flow cytometry identified a potential pharmacodynamic biomarker of ICOS agonistic effects in peripheral blood, ICOS-hi CD4 T cells, and its association with clinical outcomes was evaluated.

Patients who displayed on-treatment emergence of ICOS-hi CD4 T cells had significantly greater clinical benefit from treatment than those who did not (**Fig. 1**). The objective response rate (ORR) in patients with ICOS-hi CD4 T-cell emergence was 4/20 (20%), compared with 0 of 24 (0%) in ICOS-lo patients ($P = 0.0357$). Median PFS in the ICOS-hi CD4 T-cell group was 6.2 months (95% CI, 3.4–19.6) compared with 1.9 months (95% CI, 1.8–2.1; $P < 0.001$) in the ICOS-lo group, and the median OS reached 20.7 months (95% CI, 9.1–not estimable) in the ICOS-hi group but was only 9.0 months (95% CI, 5.4–13.6; $P = 0.0025$) in the ICOS-lo group. These differences are not explained by patients' clinical baseline characteristics, which were evenly distributed across both groups (Supplementary Table S4).

Representative flow cytometry analysis shows that a patient who achieved a confirmed RECIST v1.1 PR demonstrated emergence of ICOS-hi CD4 T cells, while one patient with confirmed RECIST v1.1 stable disease initially demonstrated the emergence of ICOS-hi CD4 T cells, but subsequently demonstrated loss of this cell population upon radiological progression (Supplementary Fig. S6A). Moreover, in a patient with best response of radiological progressive disease, no emergence was observed in peripheral blood (Supplementary Fig. S6A).

Although ICOS can also be upregulated on CD8 T cells, an ICOS-hi CD8 population was not detected, suggesting a CD4-focused mechanism of action for vopratelimab (Supplementary Fig. S6B). ICOS-hi CD4 T cells were present within the peripheral CD4 compartment at high levels and persisted over the course of treatment in patients with confirmed RECIST v1.1 PR to vopratelimab monotherapy or in combination with nivolumab ($n = 4$; Supplementary Fig. S6C).

To confirm that the observed ICOS-hi CD4 T-cell emergence was a vopratelimab-specific response [and not a PD-(L)1 inhibitor response], a companion phenotyping study was performed in 77 patients with advanced NSCLC ($N = 64$) and melanoma ($N = 12$) treated with commercially available PD-1 or PD-L1 inhibitor monotherapy, and included 6 radiological responders (19).

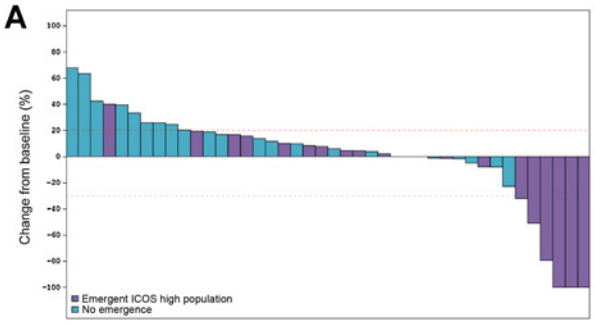

B

	ICOS-hi (n = 20)	ICOS-lo (n = 24)
RECIST 1.1 ORR, n (%) (95% CI) P = 0.0357	4 (20.0%) (5.73–43.66)	0 (0.00–14.25)
Median PFS (mo) (95% CI) P < 0.0001	6.2 (3.4–19.6)	1.9 (1.8–2.1)
Median OS (mo) (95% CI) P = 0.0025	20.7 (9.1–NE)	9.0 (5.4–13.6)

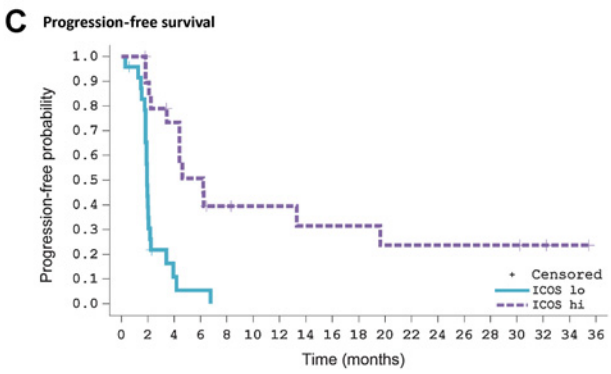

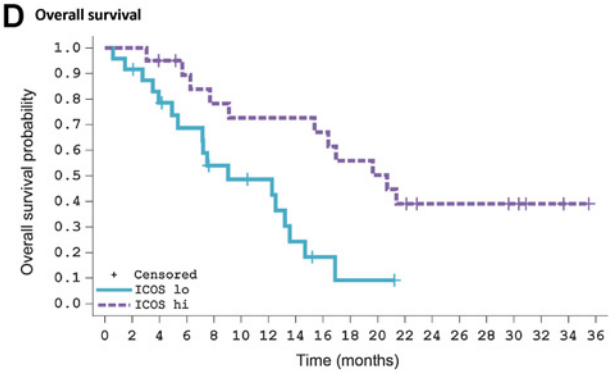

Figure 1.

Pharmacodynamic biomarker ICOS-hi CD4 T-cell emergence correlates with response and improvements in OS and PFS. A retrospective analysis was performed on 44 patients who had both evaluable longitudinal PBMC samples and were evaluable for efficacy. In all panels, patients who have ICOS-hi CD4 T-cell emergence at any timepoint are depicted in purple; patients without ICOS-hi CD4 T-cell emergence at any time are depicted in blue. **A,** Waterfall plot reflecting individual patients' maximum reduction in the sum of diameters of target tumors compared with baseline in patients with at least one postbaseline CT scan ($n = 42$). Not all patients with ≥ 30% tumor reductions are RECIST PR. **B,** Patients with emergence of ICOS-hi CD4 T cells had improved responses, PFS, and OS as compared with patients without emergence of this pharmacodynamic biomarker. **C,** Kaplan–Meier curve demonstrates improved PFS in ICOS-hi versus ICOS-lo patients. **D,** Kaplan–Meier curve demonstrating the OS benefit for patients with ICOS-hi CD4 T-cell emergence as compared with patients who are ICOS-lo. Data cutoff for all panels is July 22, 2020. ICOS, inducible costimulator; ICOS-hi, patients with an emergent CD4 T-cell population with high levels of ICOS; ICOS-lo, patients without the emergence of a CD4 T-cell population expressing high levels of ICOS; PFS, progression-free survival; ORR, overall response rate; OS, overall survival; NE, not estimable.

The emergence of ICOS-hi CD4 T cells was not observed at any on-treatment timepoint over the 6-month period assessed in any of these patients treated with single-agent PD-(L)1 inhibitors, as seen in the representative flow cytometry histogram analyses from responding patients with NSCLC in Supplementary Fig. S6D and S6E, respectively (19).

Characterization of peripheral ICOS-hi CD4 T cells

Further characterization of the 44 patients on the ICONIC trial with serially collected pretreatment and on-treatment PBMC samples and efficacy assessments demonstrated that the peripheral ICOS-hi CD4 T cells were enriched in certain CD4 T-cell subsets, including Th1, T central memory (Tcm), and follicular Th cells (Tfh), but not in regulatory T cells. In the subset of patients with emergence of the ICOS-hi CD4 T-cell population, sustained proliferation of these cells as measured by Ki-67 expression was observed with vopratelimab alone or in combination with nivolumab. This suggests a CD4-centric mechanism (Supplementary Fig. S7A), as only an early CD8 proliferation signal was identified, consistent with nivolumab pharmacodynamic activity (20). Gene expression analysis of CD4 T cells from ICOS-hi responders to vopratelimab in combination with nivolumab compared with ICOS-lo CD4 T cells from representative patients with cancer showed that gene expression profiles were significantly different between these groups (FDR-adjusted P value <0.05). As a bulk population, ICOS-hi CD4 T cells were more likely to express genes associated with cytotoxic function (perforin and granzymes), and effector T-cell activation (Supplementary Fig. S7B and S7D). Additional phenotypic profiling demonstrated no enrichment of regulatory T cells within the ICOS-hi CD4 T-cell population as cells were negative for CD25 and FOXP3 (Supplementary Fig. S7C). Further flow profiling demonstrated enrichment of subsets, including Th1, Tcm, and Tfh, which were represented as relatively equivalent fractions of the CD4 compartment (Supplementary Fig. S7D).

Identifying a predictive biomarker of response to vopratelimab

The association between a vopratelimab-specific pharmacodynamic biomarker (emergence of ICOS-hi CD4 T cells) and clinical benefit enabled a focused assessment of predictive biomarkers of response to determine whether baseline characteristics could predict for ICOS-hi CD4 T-cell emergence and therefore select for the patient population that may benefit most from vopratelimab. Various biomarkers in baseline tumor tissue were evaluated for their ability to predict the emergence of a peripheral ICOS-hi CD4 T-cell population in response to vopratelimab with or without nivolumab. In baseline tumor tissue, neither ICOS IHC nor PD-L1 IHC were found to predict the emergence of a peripheral ICOS-hi CD4 T-cell population in response to

A

TIS Biology	Gene
Antigen-presenting cell abundance	*PSMB10*
	HLA-DQA1
	HLA-DRB1
	CMKLR1
T-cell/NK-cell abundance	*HLA-E*
	NKG7
	CD8A
IFN activity	*CCL5*
	CXCL9
	CD27
	CXCR6
	IDO1
	STAT1
T-cell exhaustion	*TIGIT*
	LAG3
	CD274
	PDCD1LG2
	CD276

B

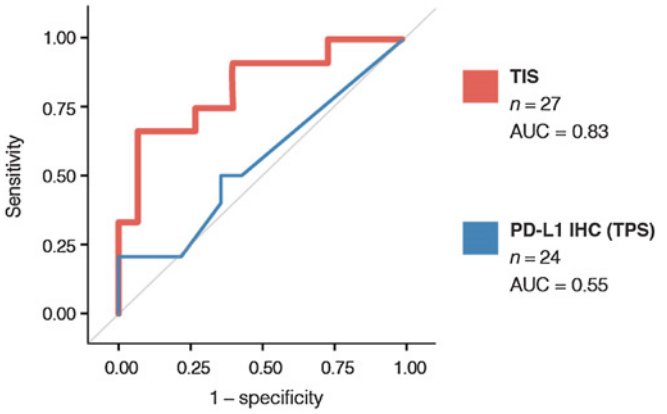

Figure 2.

Identifying TIS as a biomarker for the emergence of ICOS-hi CD4 T cells and calculating a threshold for TIS^{vopra}. Various tumor biomarkers were evaluated for their ability to predict the emergence of a peripheral ICOS-hi CD4 T-cell population in response to vopratelimab monotherapy or with nivolumab. **A,** The 18 TIS genes are associated with antigen presentation, lymphocyte abundance, IFN activity, and T-cell exhaustion, including activation of CD4 T cells. Genes highlighted in blue are involved in antigen presentation to CD4 T cells (*HLA-DRB1* and *HLA-DQA1*) and successful recruitment of T cells and antigen-presenting cells (*CCL5* and *CXCL9*). **B,** ROC curve demonstrating the ability of TIS to predict ICOS-hi CD4 T-cell emergence ($n = 27$, AUC = 0.83) and the lack of prediction by PD-L1 IHC ($n = 24$, AUC = 0.55). AUC, area under the curve; ICOS, inducible costimulator; IHC, immunohistochemistry; PD-L1, programmed death-ligand 1; ROC, receiver operating characteristic; TIS, tumor inflammation signature.

vopratelimab monotherapy or in combination with nivolumab (Supplementary Fig. S8). However, using NanoString's nCounter profiling of RNA isolated from pretreatment tumor biopsies ($n = 89$), an association was found between the TIS gene expression score (21) and emergence of ICOS-hi CD4 T cells in the 27 patients who had data for both TIS score and ICOS. The 18 TIS genes, originally demonstrated as predictive of response to anti-PD-1 therapy (16), are associated with IFNγ signaling, antigen presentation, lymphocyte and monocyte abundance, and activation of CD4 T cells and other immune cells (**Fig. 2A**). Because vopratelimab activity requires the presence of activated CD4 T cells (14), the genes included in TIS are highly relevant to vopratelimab. Patients with treatment-emergent ICOS-hi CD4 T cells had a higher median TIS score ($N = 12$, 7.9) than those in the ICOS-lo group ($N = 15$, 6.7; $P = 0.0031$, two-sided Wilcoxon two-sample exact test). ROC curve analysis determined that TIS was predictive for the emergence of ICOS-hi CD4 T cells ($n = 27$; AUC = 0.83; **Fig. 2B**). The optimal TIS threshold of 7.9 (TIS^{vopra}) for predicting this TIS-driven PD response (emergence of an ICOS-hi CD4 T-cell population) was calculated using the Youden index to optimize sensitivity and specificity. TIS^{vopra} has a positive predictive value of 89% and a negative predictive value of 78% for the emergence of the cell population.

An analysis of the correlation of TIS^{vopra} with efficacy was done on 89 patients for whom TIS^{vopra} data were available ($n = 29$ received vopratelimab, $n = 60$ received vopratelimab + nivolumab). Patients treated with vopratelimab alone and in combination with nivolumab with TIS^{vopra}-positive baseline tumor samples had better outcomes to treatment compared with those with TIS^{vopra}-negative tumor samples including RECIST responses, a higher PFS rate at 6 months and median OS. Specifically, radiological target lesion tumor reduction was greater in patients with TIS^{vopra}-positive tumors versus those with TIS^{vopra}-negative tumors (**Fig. 3A**); the ORR in TIS^{vopra}-positive patients was 14.3% (3/21; TIS score was not obtained for the 1 responder to vopratelimab monotherapy) compared with 0.0% (0/62) in TIS^{vopra}-negative ($P = 0.0145$; Supplementary Table S4). In addition, patients in the TIS^{vopra}-positive group remained on treatment longer than those in the TIS^{vopra}-negative group (**Fig. 3B**); mean (SD) treatment duration of 7.8 months (10.40) with a range of 1.2–34.8 months in TIS^{vopra}-positive versus 2.3 months (1.61) with a range of 0.2–7.9 months in the TIS^{vopra}-negative group ($P = 0.0205$). Median PFS was 2.2 months (95% CI, 2.0–4.6 months) for TIS^{vopra}-positive patients ($n = 22$) compared with 1.9 months (95% CI, 1.8–2.0 months) for TIS^{vopra}-negative patients ($n = 67$; **Fig. 3C**); the P value for PFS comparison of TIS^{vopra}-positive versus TIS^{vopra}-negative patients is 0.0002 using log-rank test, suggesting significant overall risk reduction in disease progression or death for the TIS^{vopra}-positive patients. The probability of being progression free at 6 months was 21.1% (95% CI, 6.6–41.1) for TIS^{vopra}-positive patients compared with 3.8% (95% CI, 0.7–11.4) for TIS^{vopra}-negative patients, $P < 0.0001$. The PFS rate at 9 months was 21.1% (95% CI, 6.6–41.1) for TIS^{vopra}-positive patients, while all TIS^{vopra}-negative patients discontinued prior to 9 months. An improvement was also seen in median OS, which was 16.9 months (95% CI, 9.1–21.4 months) for TIS^{vopra}-positive patients ($n = 22$) compared with 6.2 months (95% CI, 3.7–9.0 months) for TIS^{vopra}-negative patients ($n = 67$), $P = 0.0062$ (**Fig. 3D**). Finally, OS rate at 12 months since first dose was 60.7% (95% CI, 34.4–79.1) for TIS^{vopra}-

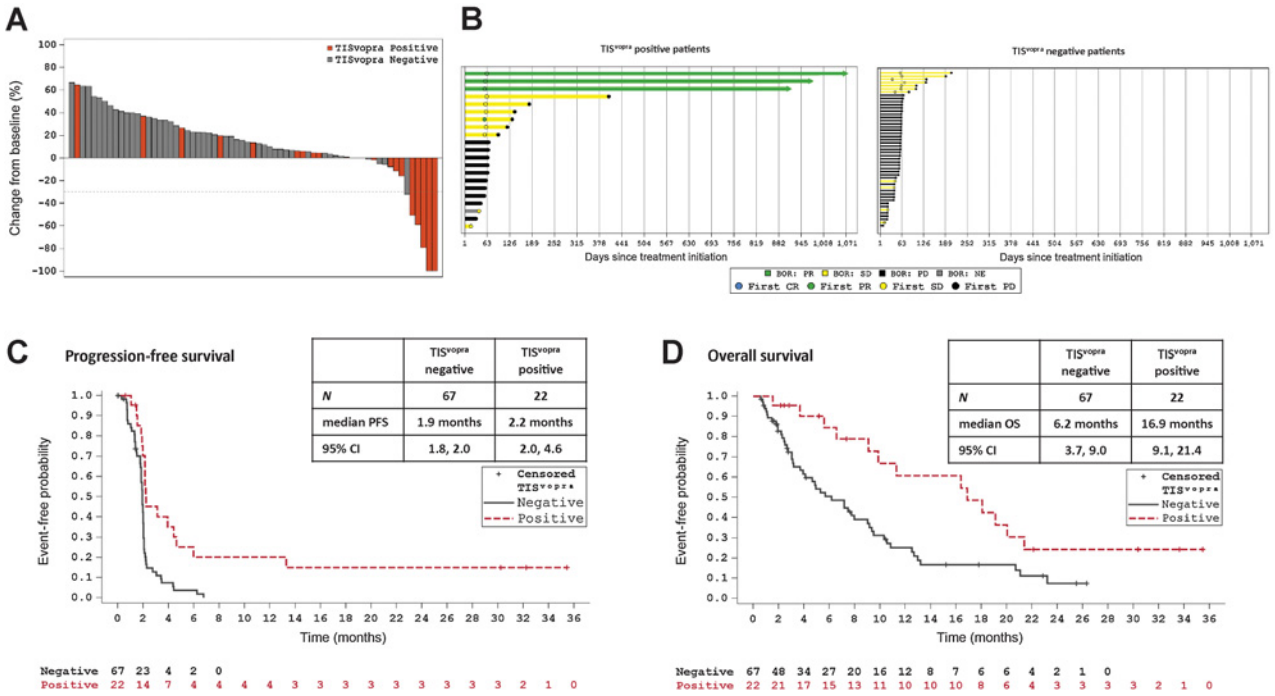

Figure 3.

TIS^{vopra} predicts tumor regression and clinical benefit. ICONIC patients treated with vopratelimab monotherapy or in combination with nivolumab who had pretreatment tumor samples that were TIS^{vopra} positive showed better outcomes to treatment than those whose tumor samples were TIS^{vopra} negative. In all panels, orange depicts TIS^{vopra}-positive patients and gray shows TIS^{vopra}-negative patients. **A,** Waterfall plot showing maximum reduction in the sum of diameters of target tumors compared with baseline in patients with at least one postbaseline CT scan who were assessed for TIS^{vopra} status ($n = 67$). **B,** Swimmer plots showing time on treatment for patients who were evaluated for TIS^{vopra} ($n = 89$). Arrows indicate patients for whom treatment is ongoing. Left, Patients who are TIS^{vopra} positive; right, patients who are TIS^{vopra} negative. BOR is evaluated using RECIST 1.1; PR is depicted in green, stable disease is depicted in yellow, PD is depicted black, NE is depicted in gray. **C,** PFS curves for TIS^{vopra}-positive versus TIS^{vopra}-negative patients, as evaluated by investigator review. An event is defined as PD or death (see Patients and Methods). **D,** OS curves for TIS^{vopra}-positive versus TIS^{vopra}-negative patients. An event is defined as death (see Patients and Methods). BOR, best overall response; CR, complete response; ICOS, inducible costimulator; PD, progressive disease; PR, partial response; RECIST, response evaluation criteria in solid tumors; SD, stable disease; TIS, tumor inflammation signature. Data cutoff for all panels is July 22, 2020.

positive patients compared with 25.1% (95% CI, 14.4–37.3) for TIS^{vopra}-negative patients, $P < 0.0001$. Although the TIS^{vopra} threshold was developed to predict emergence of ICOS-hi CD4 T cells and not OS, an additional analysis of OS was done excluding the 27 patients whose data was used to determine the TIS^{vopra} threshold. A similar trend was observed: TIS^{vopra}-positive patients ($N = 13$) demonstrated prolonged survival with a median OS of 9.9 versus 4.9 months in TIS^{vopra}-negative patients ($N = 49$), $P = 0.3055$ (Supplementary Fig. S9).

Discussion

The ICOS pathway has gained great interest in oncology as it plays an important role in memory and effector T-cell development and specific humoral immune responses; thus ICOS agonist antibodies have emerged as an active class of investigational immunotherapy agents, with multiple agents currently in clinical trial development (22). Data from chimeric Ag receptors (CAR) with ICOS intracellular binding domains demonstrated improved efficacy in solid tumor models due to an increase in persistence of CD4$^+$ and CD8$^+$ CAR T cells and effector function important for durable remissions, suggesting an important role for ICOS agonism in durability of response (22, 23). The ICONIC phase I/II study is the first trial to assess the safety, pharmacokinetics, pharmacodynamics, preliminary efficacy and predictive biomarkers of response to vopratelimab, an ICOS agonist mAb, alone and in combination with nivolumab in a heavily pretreated patient population.

Vopratelimab was well tolerated and did not impact the safety profile of nivolumab. Selection of the RP2D (0.3 mg/kg every 3 weeks) was based on sustained TE throughout the dosing period as well as safety and pharmacokinetic data. ADAs were observed, but there was no apparent difference between vopratelimab pharamcokinetic parameters determined by noncompartmental analysis for patients with and without ADA, and a concentration–response relationship between vopratelimab exposure and target engagement was established. Taken together, these data indicate that the level of ADA observed most likely did not affect the activity of vopratelimab in this study.

Treatment with vopratelimab alone or in combination with nivolumab did not result in significant tumor reductions. The significance of this study lies in the hypothesis-testing, reverse translational approach, in which blood and tumor samples were collected from patients and analyzed for biomarkers that correlated with clinical outcomes. This led to the identification of a peripheral blood pharmacodynamic biomarker, treatment-emergent ICOS-hi CD4 T cells, that provided clinical evidence of the mechanism of action of vopratelimab and was associated with clinical benefit. Emergence and persistence of this pharmacodynamic biomarker confirmed that agonism of ICOS by vopratelimab results in the proliferation and sustained

activation of ICOS-hi CD4 T cells, which include Th1, Tcm, and Tfh subsets. The combined functions of these T-cell subsets support the role of vopratelimab in eliciting both direct and durable antitumor responses of patients: Th1 cells possess direct antitumor activity, Tfh cells support B cell and cytotoxic CD8 activity, and perhaps most importantly, Tcm cells may contribute to the long durability of the antitumor responses. The emergence and persistence of these T cells in patients with advanced cancers benefiting from an ICOS agonist supports the role of ICOS in generating a comprehensive and durable immune response to cancer.

Also noteworthy, the pharmacodynamic biomarker has isolated the effects of vopratelimab from the combination partner nivolumab, a PD-1 inhibitor, enabling a vopratelimab-specific approach for the identification of the potential predictive biomarker of response, TIS^{vopra}. TIS includes genes involved in CD4 T-cell activation and has been shown to be predictive for response to PD-1 inhibitors using different thresholds (16, 21, 24). The threshold determined in this study for TIS^{vopra} is based on prediction of ICOS- hi CD4 T-cell emergence, thereby presumably exploiting prediction for PD-1 inhibition, and importantly, optimizing it directly as a predictor of the CD4 focused mechanism of action of vopratelimab. Application of TIS^{vopra} to the ICONIC data demonstrated a statistically significant improvement in clinical outcomes for TIS^{vopra}-positive patients compared with patients below the threshold. TIS has been evaluated and shown not to be prognostic in most cancers, including gastric (21, 25), supporting its use as a predictive biomarker for vopratelimab-based therapy. While not all patients will benefit from immunotherapy, we hypothesize that utilization of a predictive biomarker for vopratelimab will identify patients in whom the therapeutic mechanism is most relevant, potentially resulting in durable clinical benefit in such patients. The ability of the TIS^{vopra} biomarker signature to identify patients most likely to benefit from the combination of vopratelimab and a PD-1 inhibitor is currently being tested prospectively in a randomized phase II trial of vopratelimab plus an investigational PD-1 inhibitor JTX-4014 (pimivalimab), versus JTX-4014 alone in patients with PD-(L)1 inhibitor–naïve NSCLC (SELECT, NCT04549025). More broadly, the concept of identifying and utilizing a treatment-emergent pharmacodynamic biomarker to enable an expanded identification of patients for predictive biomarker assessments may lead to an improved means of matching the right immunotherapy with the right patient.

Limitations of the study include the low tumor response rates observed, the small number of samples evaluated for peripheral and tissue-based biomarker studies, as well as the retrospective and prospective analysis of peripheral blood samples. However, the identification of both the pharmacodynamic biomarker, treatment-emergent ICOS-hi CD4 T cells and the potential predictive biomarker, TIS^{vopra}, are intriguing findings that have led to the current clinical development program of vopratelimab, and may also be applicable to other ICOS agonists in clinical development. We believe that such a biomarker-driven strategy in early clinical drug development is necessary for the successful optimization of immunotherapy combinations, particularly as clinical approaches involving novel agents with PD-(L)1 inhibitors in broader molecularly unselected populations of patients have largely not been met with success.

Authors' Disclosures

T.A. Yap reports other support from Seagen and University of Texas MD Anderson Cancer Center; grants from Acrivon, Artios, AstraZeneca, Bayer, Beigene, BioNTech, Blueprint, BMS, Clovis, Constellation, Cyteir, Eli Lilly, EMD Serono, Forbius, F-Star, GlaxoSmithKline, Genentech, Haihe, ImmuneSensor, Ionis, Ipsen, Jounce, Karyopharm, KSQ, Kyowa, Merck, Mirati, Novartis, Pfizer, Ribon Therapeutics, Regeneron, Repare, Rubius, Sanofi, Scholar Rock, Seattle Genetics, Tesaro, Vivace, and Zenith; and personal fees from AbbVie, AstraZeneca, Acrivon, Adagene, Almac, Aduro, Amphista, Artios, Athena, Atrin, Avoro, Axiom, Baptist Health Systems, Bayer, Beigene, Boxer, Bristol Myers Squibb, C4 Therapeutics, Calithera, Cancer Research UK, Clovis, Cybrexa, Diffusion, EMD Serono, F-Star, Genmab, Glenmark, GLG, Globe Life Sciences, GSK, Guidepoint, Idience, Ignyta, I-Mab, ImmuneSensor, Institut Gustave Roussy, Intellisphere, Jansen, Kyn, MEI Pharma, Mereo, Merck, Natera, Nexys, Novocure, OHSU, OncoSec, Ono Pharma, Pegascy, PER, Pfizer, Piper-Sandler, Prolynx, Repare, resTORbio, Roche, Schrodinger, Theragnostics, Varian, Versant, Vibliome, Xinthera, Zai Labs, and ZielBio outside the submitted work. J.F. Gainor reports other support from Jounce during the conduct of the study as well as personal fees and other support from Bristol-Myers Squibb, Merck, Loxo/Lilly, Genentech/Roche, AstraZeneca, Novartis, and Blueprint and personal fees from Oncorus, Regeneron, Gilead, Moderna, Mirati, Pfizer, iTeos, Nuvalent, Karyopharm, Beigene, Silverback Therapeutics, and GlydeBio outside the submitted work; in addition, J.F. Gainor has an immediate family member who is an employee with equity in Ironwood Pharmaceuticals. M.K. Callahan reports grants from Bristol Myers Squibb and personal fees from Merck, AstraZeneca, ImmunoCore, and Moderna outside the submitted work. G.S. Falchook reports grants from Jounce during the conduct of the study as well as royalties (self) from Wolters Kluwer (2014–present); an advisory role (to institution) with Fujifilm (2018), Silicon (2020 and 2021), Navire (2021), Turning Point (2021), Predicine (2021), Inspirna (2021), and Regeneron (2021); an advisory role (self) with EMD Serono (2010 and 2011); speakers honorarium for CME from Total Health Conferencing (2019) and Rocky Mountain Oncology Society (2020); travel support (self, for work or research related to institution) from Bristol-Myers Squibb (2015), EMD Serono (2011, 2012, and 2013), Fujifilm (2018), Millennium (2013), and Sarah Cannon Research Institute; and research funding [to institution, for any trial for which G.S. Falchook has been the PI (ever) or subinvestigator (minimum last 4 years)] from 3-V Biosciences, Abbisko, AbbVie, ABL Bio, ADC Therapeutics, Accutar, Aileron, American Society of Clinical Oncology, Amgen, ARMO/Eli Lilly, Artios, AstraZeneca, BeiGene, Bioatla, Bioinvent, Biothera, Bicycle, Black Diamond, Boehringer Ingelheim, Celldex, Celgene, Ciclomed, Curegenix, Curis, Cyteir, Daiichi, DelMar, eFFECTOR, Eli Lilly, EMD Serono, Epizyme, Erasca, Exelixis, Freenome, Fujifilm, Genmab, GlaxoSmithKline, Hutchison MediPharma, IGM Biosciences, Ignyta, ImmunoGen/MacroGenics, Incyte, Jacobio, Jounce, Kolltan, Loxo/Bayer, MedImmune, Millennium, Merck, miRNA Therapeutics, Molecular Templates, National Institutes of Health, Navire, NiKang, Novartis, OncoMed, Oncorus, Oncothyreon, Poseida, Precision Oncology, Prelude, PureTech, Pyramid, RasCal, Regeneron, Relay, Rgenix, Ribon, Samumed, Sapience, Seagen, Silicon, Simcha, Sirnaomics, Strategia, Syndax, Synthorx/Sanofi, Taiho, Takeda, Tarveda, Teneobio, Tesaro, Tocagen, Turning Point, University of Texas MD Anderson Cancer Center, Vegenics, and Xencor. R.K. Pachynski reports personal fees from Jounce during the conduct of the study as well as personal fees from AstraZeneca, Dendreon, Pfizer/Astellas, WalkingFish Therapeutics, and Blue Earth Diagnostics and nonfinancial support from Genentech/Roche, BMS, Exelixis, Janssen, and Pharmacyclics outside the submitted work. P. LoRusso reports personal fees from AbbVie, Agios, Five Prime, GenMab, and Halozyme and other support from Roche-Genentech, Genentech, CytomX, Takeda, SOTIO, Cybrexa, Agenus, Tyme, IQVIA, TRIGR, Pfizer, ImmunoMet, Black Diamond, GlaxoSmithKline, QED Therapeutics, AstraZeneca, EMD Serono, Shattuck, Astellas, Salarius, Silverback, MacroGenics, Kyowa Kirin, Kineta, Zentalis, Molecular Templates, ABL Bio, SK Life Science, STCube, Bayer, I-Mab, Seagen, imCheck, Relay Therapeutics, Stemline, Compass BADX, Mekanist, and Mersana Therapeutic outside the submitted work. S. Kummar reports other support from Jounce during the conduct of the study as well as other support from Bayer, Mundibiopharma, Gilead, Oxford BioTherapeutics, Pathomiq, Cadila Pharmaceuticals, Arxeon, Harbour Biomed, Varian, and Springworks Therapeutics outside the submitted work. G.T. Gibney reports personal fees from Merck, Regeneron, Bristol Myers Squibb, Genentech, Novartis, Eisai, Exicure, and Sapience Therapeutics and other support from Exelixis and Lucerno Dynamics outside the submitted work. H.A. Burris reports grants from Jounce Therapeutics during the conduct of the study as well as grants from Roche/Genentech, Bristol-Myers Squibb, Incyte, AstraZeneca, MedImmune, Macrogenics, Novartis, Boehringer Ingelheim, Lilly, SeaGen, Merck, Agios, Moderna Therapeutics, CytomX Therapeutics, GlaxoSmithKline, Verastem, Tesaro, BioMed Valley Discoveries, TG Therapeutics, Vertex, eFFECTOR Therapeutics, Janssen, Gilead Sciences, BioAtla, CicloMed, Harpoon Therapeutics, Arch, Arvinas, Revolution Medicines, Array BioPharma, Bayer, BIND Therapeutics, Kymab, miRNA Therapeutics, Pfizer, Takeda/Millennium, Foundation Medicine, EMD Serono, ARMO Biosciences, CALGB, Hengrui Therapeutics, Infinity Pharmaceuticals, XBiotech, Zymeworks, Coordination

Pharmaceuticals, NGM Biopharmaceuticals, Gossamer Bio, Ryvu Therapeutics, BioTheryX, and AbbVie and other support from Daiichi Sankyo, Pfizer, Bayer, GRAIL, Novartis, Vincerx Pharma, AstraZeneca, Incyte, Boehringer Ingelheim, Bristol Myers Squibb, and TG Therapeutics outside the submitted work. S.S. Tykodi reports nonfinancial and other support from Jounce Therapeutics during the conduct of the study as well as other support from Merck, Nektar Therapeutics, Pfizer, Clinigen, Bristol Myers Squibb, Exelixis, and AVEO Oncology and personal fees from Bristol Myers Squibb, Exelixis, Merck, Intellisphere, Cancer Network, and PSL Group Services outside the submitted work; in addition, S.S. Tykodi has a provisional patent application pending for tumor antigen 5T4 specific T-cell receptor gene sequences. O.E. Rahma reports personal fees from AstraZeneca, Boehringer Ingelheim, Sobi, Genentech, Bayer, GSK, ImVAX, and Maverick Therapeutic outside the submitted work; in addition, O.E. Rahma has a patent for methods of using pembrolizumab and trebananib pending. T.Y. Seiwert reports grants from Jounce Therapeutics during the conduct of the study as well as grants and personal fees from Merck/MSD and Nanobiotix; grants from BMS, Regeneron, Genentech/Roche, and AstraZeneca; and personal fees from Innate, Coherus Biosciences, Sanofi, BostonGene, and Syneos/BioNTech outside the submitted work. K.P. Papadopoulos reports other support from Jounce during the conduct of the study as well as other support from AbbVie, Medimmune, Daiichi Sankyo, Regeneron, Amgen, Calithera Biosciences, Incyte, Merck, Peloton Therapeutics, ADC Therapeutics, 3D Medicines, Syros Pharmaceuticals, Mersana, Mabspace Biosciences, Bayer, Anheart, F-star, Linnaeus, Mirati Therapeutics, Tempest Therapeutics, Treadwell Therapeutics, Lilly, Pfizer, BioNTech, Bicycle Therapeutics, and Kezar Life Sciences and personal fees from Basilia, Bicycle Therapeutics, and Turning Point Therapeutics outside the submitted work. H. Park reports grants and nonfinancial support from Jounce during the conduct of the study as well as grants (to institution) from Adlai Nortye USA, Alpine Immune Sciences, Ambrx, Amgen, Aprea Therapeutics AB, Array BioPharma, Bayer, BeiGene, BJ Bioscience, Bristol-Myers Squibb, Daiichi Pharmaceutical, Eli Lilly, Elicio Therapeutics, EMD Serono, Exelixis, Genentech, Gilead Sciences, GlaxoSmithKline, Gossamer Bio, Hoffman-LaRoche, Hutchison MediPharma, ImmuneOncia Therapeutics, Incyte, Mabspace Biosciences, MacroGenics, Medimmune, Merck, Mirati Therapeutics, Novartis Pharmaceuticals, Oncologie, Pfizer, PsiOxus Therapeutics, Puma Biotechnology, Regeneron Pharmaceuticals, RePare Therapeutics, Seattle Genetics, Synermore Biologics, Taiho Pharmaceutical, TopAlliance Biosciences, Turning Point Therapeutics, Vedanta Biosciences, and Xencor Inc outside the submitted work. A. Hanson reports personal fees and other support from Jounce Therapeutics outside the submitted work; in addition, A. Hanson has a patent for methods and compositions for the treatment of cancer and infectious diseases (WO-2020086802-A1) issued. Y. Hashambhoy-Ramsay reports other support from Jounce Therapeutics outside the submitted work; in addition, Y. Hashambhoy-Ramsay has a patent (WO2021146303) pending. L. McGrath reports personal fees from Jounce Therapeutics and AstraZeneca outside the submitted work; in addition, L. McGrath has patents (US Patent App. 17/286,104 and US Patent App. 17/171,866) pending to Jounce Therapeutics. E. Hooper reports personal fees from Jounce Therapeutics during the conduct of the study as well as personal fees from Jounce Therapeutics outside the submitted work. X. Xiao reports personal fees from Jounce Therapeutics during the conduct of the study. H. Cohen is a current employee of Bicycle Therapeutics (took position after work was completed). M. Fan reports patents (US20190367613A1 and WO2020086802A1) pending to Jounce Therapeutics; in addition, M. Fan is a former employee of Jounce Therapeutics. D. Felitsky reports personal fees from Jounce Therapeutics during the conduct of the study. R. McComb reports other support from Takeda Pharmaceuticals outside the submitted work. K. Brown reports other support from Jounce Therapeutics during the conduct of the study as well as other support from Jounce Therapeutics outside the submitted work. A. Sepahi reports other support from Jounce Therapeutics during the conduct of the study as well as other support from Jounce Therapeutics outside the submitted work. J. Jimenez reports other support from Jounce Therapeutics during the conduct of the study as well as other support from Jounce Therapeutics outside the submitted work. J. Baeck reports other support from Jounce Therapeutics during the conduct of the study as well as other support from Jounce Therapeutics outside the submitted work. H. Laken reports other support from Jounce Therapeutics outside the submitted work. R. Murray reports other support from Jounce Therapeutics during the conduct of the study as well as other support from Jounce Therapeutics outside the submitted work; in addition, R. Murray is CEO of Jounce Therapeutics. E. Trehu reports other support from Jounce Therapeutics during the conduct of the study as well as other support from Jounce Therapeutics outside the submitted work. C.J. Harvey reports personal fees from Jounce Therapeutics during the conduct of the study; in addition, C.J. Harvey has patents (11,292,840 and 10,968,277) issued. No disclosures were reported by the other authors.

Authors' Contributions

T.A. Yap: Investigation, writing–review and editing. **J.F. Gainor:** Investigation. **M.K. Callahan:** Investigation. **G.S. Falchook:** Investigation. **R.K. Pachynski:** Investigation. **P. LoRusso:** Investigation. **S. Kummar:** Investigation. **G.T. Gibney:** Investigation. **H.A. Burris:** Investigation. **S.S. Tykodi:** Investigation. **O.E. Rahma:** Investigation. **T.Y. Seiwert:** Investigation. **K.P. Papadopoulos:** Investigation. **M. Blum Murphy:** Investigation. **H. Park:** Investigation. **A. Hanson:** Investigation. **Y. Hashambhoy-Ramsay:** Formal analysis, investigation. **L. McGrath:** Investigation. **E. Hooper:** Supervision, investigation. **X. Xiao:** Software, validation. **H. Cohen:** Formal analysis. **M. Fan:** Investigation. **D. Felitsky:** Investigation. **C. Hart:** Supervision. **R. McComb:** Supervision. **K. Brown:** Formal analysis, methodology. **A. Sepahi:** Formal analysis, validation. **J. Jimenez:** Data curation, writing–original draft, project administration, writing–review and editing. **W. Zhang:** Formal analysis. **J. Baeck:** Supervision. **H. Laken:** Formal analysis, writing–review and editing. **R. Murray:** Conceptualization, writing–review and editing. **E. Trehu:** Conceptualization, resources, data curation, formal analysis, supervision, investigation, writing–review and editing. **C.J. Harvey:** Conceptualization, data curation, formal analysis, investigation, methodology, writing–original draft.

Acknowledgments

The authors would like to thank the participants in this trial and their families. Writing assistance was provided by Kristin O'Malley, Edward Stack, and Anna Kreshock at Jounce Therapeutics. The ICONIC trial and the preparation of this article were funded by Jounce Therapeutics, Inc. T.A. Yap acknowledges the MD Anderson Cancer Center Support grant (NIH/NCI P30 CA016672), Clinical Translational Science Award 1UL1 TR003167, and the Cancer Prevention Research Institute of Texas (CPRIT) Precision Oncology Decision Support Core (RP150535).

The costs of publication of this article were defrayed in part by the payment of page charges. This article must therefore be hereby marked *advertisement* in accordance with 18 U.S.C. Section 1734 solely to indicate this fact.

Received November 30, 2021; revised March 14, 2022; accepted May 2, 2022; published first May 5, 2022.

References

1. Schmidt EV. Developing combination strategies using PD-1 checkpoint inhibitors to treat cancer. Semin Immunopathol 2019;41:21–30.
2. Yap TA, Parkes EE, Peng W, Moyers JT, Curran MA, Tawbi HA. Development of immunotherapy combination strategies in cancer. Cancer Discov 2021;11:1368–97.
3. Jenkins RW, Barbie DA, Flaherty KT. Mechanisms of resistance to immune checkpoint inhibitors. Br J Cancer 2018;118:9–16.
4. Klempner SJ, Fabrizio D, Bane S, Reinhart M, Peoples T, Ali SM, et al. Tumor mutational burden as a predictive biomarker for response to immune checkpoint inhibitors: a review of current evidence. Oncologist 2020;25:e147–59.
5. Hutloff A, Dittrich AM, Beier KC, Eljaschewitsch B, Kraft R, Anagnostopoulos I, et al. ICOS is an inducible T-cell co-stimulator structurally and functionally related to CD28. Nature 1999;397:263–6.
6. Simpson TR, Quezada SA, Allison JP. Regulation of CD4 T cell activation and effector function by inducible costimulator (ICOS). Curr Opin Immunol 2010;22:326–32.
7. Alves Costa Silva C, Facchinetti F, Routy B, Derosa L. New pathways in immune stimulation: targeting OX40. ESMO Open 2020;5:e000573.
8. Mcadam AJ, Greenwald RJ, Levin MA, Chernova T, Malenkovich N, Ling V, et al. ICOS is critical for CD40-mediated antibody class switching. Nature 2001;409:102–5.

9. Metzger TC, Long H, Potluri S, Pertel T, Bailey-Bucktrout SL, Lin JC, et al. ICOS promotes the function of CD4+ effector T cells during anti-OX40-mediated tumor rejection. Cancer Res 2016;76:3684–9.
10. Suh W-K, Tafuri A, Berg-Brown NN, Shahinian A, Plyte S, Duncan GS, et al. The inducible costimulator plays the major costimulatory role in humoral immune responses in the absence of CD28. J Immunol 2004;172: 5917–23.
11. Vidric M, Suh W-K, Dianzani U, Mak TW, Watts TH. Cooperation between 4–1BB and ICOS in the immune response to influenza virus revealed by studies of CD28/ICOS-deficient mice. J Immunol 2005;175:7288–96.
12. Hui E, Cheung J, Zhu J, Su X, Taylor MJ, Wallweber HA, et al. T cell costimulatory receptor CD28 is a primary target for PD-1-mediated inhibition. Science 2017;355:1428–33.
13. Carthon BC, Wolchok JD, Yuan J, Kamat A, Ng Tang DS, Sun J, et al. Preoperative CTLA-4 blockade: tolerability and immune monitoring in the setting of a presurgical clinical trial. Clin Cancer Res 2010;16:2861–71.
14. Hanson A, Elpek K, Duong E, Shallberg L, Fan M, Johnson C, et al. ICOS agonism by JTX-2011 (vopratelimab) requires initial T cell priming and Fc cross-linking for optimal T cell activation and anti-tumor immunity in preclinical models. PLoS One 2020;15:e0239595.
15. Michaelson JS, Harvey C, Elpek K, Duong E, Shallberg L, Wallace M, et al. Preclinical assessment of JTX-2011, an agonist antibody targeting ICOS supports evaluation in ICONIC clinical trial. [abstract]. In: Proceedings of the Annual Meeting of the American Association for Cancer Research; 2017; Washington DC.
16. Ayers M, Lunceford J, Nebozhyn M, Murphy E, Loboda A, Kaufman DR, et al. IFN-gamma-related mRNA profile predicts clinical response to PD-1 blockade. J Clin Invest 2017;127:2930–40.
17. Kaplan EL, Meier P. Nonparametric estimation from incomplete observations. J Am Stat Assoc 2958:457–81.
18. Kamphorst AO, Pillai RN, Yang S, Nasti TH, Akondy RS, Wieland A, et al. Assessment of nivolumab benefit-risk profile of a 240-mg flat dose relative to a 3-mg/kg dosing regimen in patients with advanced tumors. Ann Oncol 2017;28: 2002–8.
19. Danaher P, Warren S, Lu R, Samayoa J, Sullivan A, Pekker I, et al. Emergence of an ICOS hi CD4 T cell subset correlates with tumor reductions in subjects treated with the ICOS agonist antibody JTX-2011, in Abstract presented at: Society for Immunotherapy of Cancer (SITC) Annual Meeting; November 7–11, 2018; Washington, DC; 2018.
20. Kamphorst AO, Pillai RN, Yang S, Nasti TH, Akondy RS, Wieland A, et al. Proliferation of PD-1+ CD8 T cells in peripheral blood after PD-1-targeted therapy in lung cancer patients. Proc Natl Acad Sci U S A 2017;114:4993–8.
21. Danaher P, Warren S, Lu R, Samayoa J, Sullivan A, Pekker I, et al. Pan-cancer adaptive immune resistance as defined by the Tumor Inflammation Signature (TIS): results from The Cancer Genome Atlas (TCGA). J Immunother Cancer 2018;6:63.
22. Guedan S, Posey AD, Shaw C, Wing A, Da T, Patel PR, et al. The rationale behind targeting the ICOS-ICOS ligand costimulatory pathway in cancer immunotherapy. ESMO Open 2020;5:e000544.
23. Damotte D, Warren S, Arrondeau J, Boudou-Rouquette P, Mansuet-Lupo A, Biton J, et al. Enhancing CAR T cell persistence through ICOS and 4–1BB costimulation. JCI Insight 2018;3:e96976.
24. Damotte D, Warren S, Arrondeau J, Boudou-Rouquette P, Mansuet-Lupo A, Biton J, et al. The tumor inflammation signature (TIS) is associated with anti-PD-1 treatment benefit in the CERTIM pan-cancer cohort. J Transl Med 2019;17:357.
25. Rha SY, Ku GY, Kim HS, Chung HC, Amlashi FG, Maru DM, et al. PD-L1 expression and T-cell inflamed gene expression profile (GEP) in Korean and US patients (PTS) with advanced gastric cancer (GC). Ann Oncol 2018;29: viii205–viii270.